Structure and Spectroscopy of Metallo-Lactamase Active Sites

Hillary S. R. Gilson and Morris Krauss*

Contribution from the Center for Advanced Research in Biotechnology, 9600 Gudelsky Drive, Rockville, Maryland 20850

Received February 12, 1999

Abstract: This study clarifies the relationship between the active-site geometry of the bimetallic enzyme, zinc-β-lactamase, and the electronic spectra of the cobalt-substituted enzyme. Ab initio quantum methods were used to study both the structure and the spectroscopy of the active sites of metallo-β-lactamases. Theoretically optimized structures for the cobalt-substituted enzyme indicate that the coordination number of the two cobalt atoms remains the same as those of the zinc atoms in the crystal structure. Transition energies and intensities for the bimetallic active site were calculated by multiconfiguration self-consistent-field methods and identified with a metal center. The visible spectrum line positions and intensities calculated using correlation energy corrections derived from second-order perturbation calculations on model systems were in good agreement with the experimental data, demonstrating that the first shell of ligands determines the spectra. Visible transition energies are predicted at both metal centers, but the calculated intensities suggest that contributions from the four-coordinate site dominate the visible spectrum. The charge-transfer excitation from the cysteine to the open-shell cobalt cation results in at least 20 ligand-to-metal charge-transfer (LMCT) lines. The lowest two energy transitions are assigned to the observed 330-nm absorption, which is usually attributed experimentally to the entire LMCT transition. However, the intensities of the higher energy LMCT transitions are predicted to be much more intense.

Introduction

Metallo-β-lactamases produced by bacterial pathogens hydrolyze a wide variety of antibiotics, including penicillins, cephalosporins, and carbapenems.[1] These lactamases are native zinc enzymes but are also active with other transition metals, such as cobalt, manganese, and cadmium.[2] The X-ray structure of the zinc-β-lactamase from *B. fragilis*, which is highly active against all classes of lactam antibiotics, was determined recently to have a bimetallic active site with a bridging water or hydroxide ion.[3] One zinc site resembles the active site of carbonic anhydrase (CA), because it possess three histidine ligands (H99, H101, H162) and a bridging hydroxide ion. This site is referred to as the CA side of the active site. The zinc on the other site, referred to as the cysteine side, is bound to five ligands: an aspartate (D103), a cysteine (C181), a histidine (H223), a water (Wat2), and the bridging hydroxide ion.

The active-site properties of zinc-containing enzymes are often examined by replacing the optically inactive zinc atom with optically active cobalt, because cobalt has comparable, but not identical, structural and reactive behavior to zinc. The resulting UV−visible absorbance spectrum can be interpreted to yield information about the coordination number of the metal and the nature of the ligated residues. Using cobalt, however, to deduce the structure of a zinc site may not always lead to straightforward answers, since cobalt has a greater tendency to form a five-coordinate complex than does zinc.[4,5] A recent effort to characterize the lactamase active site from *B. fragilis* concluded that each zinc must possess either five or six first-shell ligands.[6] It was further suggested that the active-site cysteine is bound to the zinc with the three histidine ligands. Both of these interpretations followed from the low intensity of the visible spectra and were based upon empirical rules correlating intensity to coordination number.[7,8] Electronic transitions are forbidden between the atomic states of the cobalt cation but become allowed due to the lower symmetry in the molecule. Cobalt has been used also to probe the active site of the metallo-lactamase from *B. cereus*.[9−11] The visible spectrum is more intense in this case, and the active site was predicted to have the form of a distorted tetrahedron. For some time it was believed that *B. cereus* functioned as a single zinc enzyme. However, the very recent high-resolution structures of the zinc lactamase from *B. cereus* (1bme, 1bc2) show that the active site contains two zinc atoms[12,13] and that these zincs are coordinated by the same ligands as those in *B. fragilis*. If the spectrum is dominated by first-shell interactions, one would predict that the spectrum of the lactamase from *B. cereus* would

(1) Felici, A.; Amicosante, G.; Orator, A.; Strom, R.; Ledent, P.; Joris, B.; Fanuel, L.; Frère, J.-M. *Biochem. J.* **1993**, *291*, 151−155.
(2) Davies, R. B.; Abraham, E. P. *Biochem. J.* **1974**, *143*, 129−135.
(3) Concha, N. O.; Rasmussen, B. A.; Bush, K.; Herzberg, O. *Structure* **1996**, *4*, 823−836.
(4) Garmer, D. R.; Krauss, M. *J. Am. Chem. Soc.* **1993**, *115*, 10247−10257.
(5) Kremer-Aach, A.; Klaui, W.; Strerath, A.; Wunderlich, H.; Mootz, D. *Inorg. Chem.* **1997**, *36*, 1552−1563.
(6) Crowder, M. W.; Wang, Z.; Franklin, S. L.; Zovinka, E. P.; Benkovic, S. J. *Biochemistry* **1996**, *35*, 12126−12132.
(7) Bertini, I.; Luchinat, C. *Advances in Inorganic Biochemisty*; Eichorn, G. L., Marzilli, L. G., Eds.; Elsevier: New York, 1984; Vol. 6, pp 71−111.
(8) Elgren, T. E.; Ming, L. J.; Que, L., Jr. *Inorg. Chem.* **1994**, *33*, 891−894.
(9) Baldwin, G. S.; Galdes, A.; Hill, H. A. O.; Waley, S. G.; Abraham, E. P. *J. Inorg. Biochem.* **1980**, *13*, 189−204.
(10) Bicknell, R.; Schäffer, A.; Waley, S. G.; Auld, D. S. *Biochemistry* **1986**, *25*, 7208−7215.
(11) Orellano, E. G.; Girardini, J. E.; Cricco, J. A.; Cerccarelli, E. A.; Vili, A. J. *Biochemistry* **1998**, *37*, 10173−10180.
(12) Carfi, A.; Duée, E.; Galleni, M.; Frère, J.-M.; Dideberg, O. *Acta Crystallogr.* **1998**, *D54*, 313−323.
(13) Fabiane, S. M.; Sohi, M. K.; Wan, T.; Payne, D. J.; Bateson, J. H.; Mitchell, T.; Sutton, B. J. *Biochemistry* **1998**, *37*, 12404−12411.

10.1021/ja990459x CCC: $18.00
Published on Web 07/16/1999

Table 1. Some First Row Transition Metals' Ionization Potentials: M(I) to M(II)[a]

atom	MCSCF	MCQDPT	EXP(34)
Mn	14.87	15.44	15.64
Fe	15.32	15.91	16.18
Co	14.32	17.00	17.05
Ni	15.14	18.34	18.15
Cu	17.39	20.80	20.29
Zn	14.70	17.95	17.96

[a] Energies are in electronvolts.

be the same as that from *B. fragilis*. However, only the spectrum from the lactamase of *B. cereus*[9−11] appeared to be consistent with the crystal structures. The *B. fragilis* study has very recently been repeated,[14] and the resulting spectrum is, in fact, very similar, if not identical, to that of *B. cereus*. It is also interesting to note that the visible spectra of these lactamases are very similar to that of carbonic anhydrase,[15] indicating that the spectrum from the CA side of the enzyme dominates in the visible region.

The issues addressed by this paper are as follows: Is it possible that substituting cobalt for zinc recruits additional waters to the first shell, altering the coordination number and thus the spectral intensities? Do interactions between the two metal sites and the presence of ionic ligands alter the correlation of peak intensity and coordination number that is empirically observed? What effect does the presence of the cysteine have on the visible spectrum at either zinc site? Can one determine the protonation state of the active-site aspartic acid on the basis of the spectrum? What are the similarities or differences between the spectra associated with the CA and the cysteine sites of the active site? The interrelation between the sites is examined theoretically, and the universality of the results for all zinc lactamases is considered.

Methods

Energy-gradient-optimized structures were obtained at the Hartree−Fock level for zinc-containing structures and at the restricted, open-shell Hartree−Fock (ROHF) level for cobalt-containing structures using the GAMESS code.[16] Optimizations were done in vacuo with no constraints. Effective core potentials (ECPs) were used to replace all core electrons.[17,18] The CEP-31G basis set is used with the 3s, 3p, and 3d orbitals of the transition metals retained for the all-electron calculations. Although the basis is designated double-ζ since no additional polarization functions are used for the first-row elements, the transition metal 3d orbitals are represented with three 3d orbitals.

The excitation energies were first calculated at the CAS multiconfiguration self-consistent-field (MCSCF) level using the minimum active space required for spin and angular momentum coupling of all d electrons and ligand orbitals which couple into the metal. CAS-MCSCF calculations were followed, when possible, by a second-order perturbation electron correction, MCQDPT,[19] to correlate the ligand and the spd orbitals of the metal. The MCQDPT correction is necessary to correct the ionization potential of Co(II) to Co(I) during UV charge transfer (see Table 1). The atomic results are very accurate and therefore verify that the basis set and the approach to choosing the active space are appropriate for these calculations. The minimal active space for atomic Co(II) is clearly seven electrons in five orbitals, and this is the active space used to obtain the results in Table 1. Defining the minimal active space, however, becomes more complicated when the metal is surround by a variety of ligands, many of which can transfer charge. The possible active spaces for the lactamase systems were tested with MCSCF calculations on a six-coordinate model complex consisting of Co(II), methyl sulfide, and five waters. All calculations were for high-spin atoms, which are then coupled to high spin for two cobalt ions in the active site. We found that the minimal active space needed to span the d orbitals was 11 electrons in seven orbitals. A valence orbital also was needed to accommodate the charge transfer from the cysteine into the 4s and 4p orbitals of the cobalt. To ensure that the full d orbital space would be spanned in the lactamase model, an additional orbital and two electrons were added. However, this additional orbital proved to be unnecessary, and the results did not change when the orbital was removed from the active space.

CAS-MCSCF and MCQDPT calculations on non-lactamase complexes were done with fully optimized geometries. However, the coordinates for the heavy atoms of the lactamase models used in the CAS-MCSCF calculations were obtained from the coordinates of the metallo-β-lactamase from *B. fragilis*, 1znb.[3] Hydrogens were added to the PDB coordinates and optimized, keeping the heavy atoms fixed, with Gaussian 94[20] and a 3-21G basis set. The amino acid ligands were replaced by smaller models in order to make the calculations tractable. Histidine was modeled as ammonia, methylamine, methylene imine, or imidazole. The cysteine was replaced by a methyl sulfide and the aspartic acid by an acetate. Previous work on the hydration properties of cobalt has shown that expanding the basis set has a small effect on the excitation energies.[21] Oscillator strengths for the transitions were calculated using the length (dipole) form from the CAS-MCSCF orbitals.

Results

Geometry Optimizations. One concern with using the cobalt spectrum to derive information about the zinc enzyme is that the coordination numbers for cobalt and zinc in the lactamase active site may differ. To investigate this possibility, both the zinc and the cobalt active sites were optimized with two extra waters in the active site. About 100 iterations of optimization were performed. The initial water positions are those of Wat5 and Wat420 in the crystal structure 1znb. Wat5 is 3.5 Å from the zinc on the CA side, and Wat420 is 4.3 Å from the zinc on the cysteine side. The active-site geometries do not change much during the course of the optimization, and both the zincs and cobalts maintain their initial coordination numbers. During the optimization, Wat5 forms hydrogen bonds to Wat2, Wat1, and Wat420, but there is very little change in the side-chain conformations (Figure 1, hydrogens and hydrogen bonds are not shown). The resulting metal−metal distance for both zinc and cobalt is 3.7 Å. To further confirm that the coordination number of the CA side cobalt is the same as that of the zinc, another optimization in which Wat5 was moved to a position 3.36 Å from the cobalt on the CA side was performed. At this position, Wat5 is coordinated to the cobalt. After about 10 iterations of optimization, Wat5 broke its bond to the cobalt, and within 40 iterations it formed a hydrogen bond to Wat1. At this point, the optimization was stopped. These calculations

(14) Wang, Z.; Benkovic, S. J. *J. Biol. Chem.* **1998**, *273*, 22402−22408.
(15) Coleman, J. E.; Coleman, R. V. *J. Biol. Chem.* **1972**, *247*, 4718−4728.
(16) Schmidt, M. W.; Baldridge, K. K.; Boatz, J. A.; Elbert, S. T.; Gordon, M. S.; Jensen, J. H.; Koseki, S.; Matsunaga, N.; Nguyen, K. A.; Su, S.; Windus, T. L.; Dupuis, M.; Montgomery, J. A. *J. Comput. Chem.* **1993**, *14*, 1347−1363.
(17) Stevens, W. J.; Basch, H.; Krauss, M. *J. Chem. Phys.* **1984**, *81*, 6026−6033.
(18) Stevens, W.J.; Krauss, M.; Basch, H.; Jasien, P. G. *Can. J. Chem.* **1992**, *70*, 612−630.
(19) Nakano, H. *J. Chem. Phys.* **1993**, *99*, 7983−7992.
(20) Frisch, M. G.; Trucks, G. W.; Schlegel, H. B.; Gill, P. M. W.; Johnson, B. G.; Robb, M. A.; Cheeseman, J. R.; Keith, T. A.; Petersson, G. A.; Montgomery, J. A.; Raghavachari, K.; Al-Laham, M. A.; Zakrzewski, V. G.; Ortiz, J. V.; Foresman, J. B.; Cioslowski, J.; Stefanov, B. B.; Nanayakkara, A.; Challacombe, G.; Peng, C. Y.; Ayala, P. Y.; Chen, W.; Wond, M. W.; Andres, J. L.; Replogle, E. S.; Gomperts, R.; Martin, R. L.; Fox, D. J.; Binkley, J. S.; Defrees, D. J.; Baker, J.; Stewart, J. P.; Head-Gordon, M.; Gonzalez, C.; Pople, J. A. *Gaussian 94*; Gaussinc, Inc.: Pittsburgh, PA, 1995.
(21) Gilson, H. S. R.; Krauss, M. *J. Phys. Chem.* **1998**, *102*, 6525−6532.

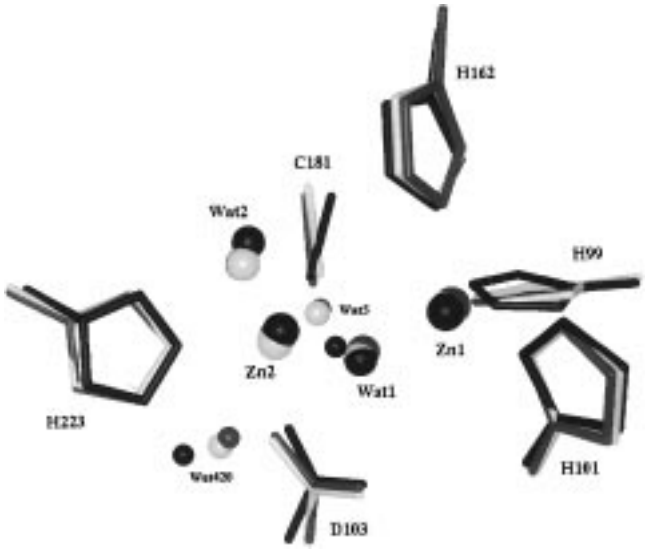

Figure 1. Comparison of the active-site structures of the metallo-β-lactamases from *B. fragilis*, 1znb (black) with the optimized structures with zinc (dark gray) and cobalt (light gray). The image was generated with VMD[25] and rendered with Raster3D.[26]

suggest that the coordination properties of cobalt in this enzyme are the same as those of zinc. Therefore, the spectrum of the cobalt-substituted enzyme should accurately reflect the properties of the native zinc enzyme.

Spectroscopy. (i) Model Complexes. Table 2 shows the excitation energies and oscillator strengths for six-coordinate, five-coordinate, and four-coordinate complexes consisting of a Co(II) ion with a methyl sulfide ion and with the remaining coordination sites occupied with waters. The geometries of the complexes were optimized before the transition energies were calculated. These calculations were done in order to investigate the effect of a charged ligand, and thus of charge transfer, on the empirically established correlation between oscillator strength and coordination number.[7] As can been seen in Table 3, the oscillator strengths of the visible transitions (states 8, 9, and 10) do correlate with the coordination number. Thus, the weakest transitions are seen in six-coordinate complexes, and the strongest transition are seen in four-coordinate complexes,[7] with the oscillator strengths increasing by about an order of magnitude with each decrease in the coordination number. This agrees qualitatively with the rule that the peak intensities will vary with the coordination number.[7] The calculated difference in the oscillator strength between the five- and six-coordinate species is larger here than is predicted empirically.[8] However, the observed transitions are all very broad, and it is difficult to relate the peak intensities quantitatively to the calculated oscillator strengths which represent the integrated area of the peak. A hexacoordinate complex with perfect symmetry will have zero oscillator strength because the transitions are symmetry forbidden. This hexacoordinate complex, however, is substantially distorted from octahedral symmetry due to the ligated methyl sulfide ligand. Electronically, the wave function behaves as if it has octahedral symmetry for the metal orbitals; however, the lowering of the symmetry provides the fields that will mix p and f components into the wave function, increasing the transition probability from zero.

Large ligand-to-metal charge-transfer (LMCT oscillator strengths are expected for all complexes since the charge-transfer transitions are, by their nature, not atomic in character. There are many LMCT states, the lowest seven of which are calculated for these complexes. These charge-transfer excited states extend well into the ultraviolet and have large oscillator strengths. As shown in Table 1, it is necessary to do these calculations at the MCQDPT level. Since it is not yet possible to do an MCQDPT calculation on the full active site, calculations on the methyl sulfide−water complexes were done at both the CAS-MCSCF and the MCQDPT levels and are used to indicate how both the visible and LMCT transition energies will shift when correlation is included. The five-coordinate complex is most relevant, since the cysteine side metal is five-coordinate. The first two LMCT transitions are shifted to the red by about 3500 cm^{-1} from the MCSCF to the MCQDPT excitation energy, and the others are shifted to the red by 1000−2000 cm^{-1}. Since the ionization potential of Co(I) is in error at the MCSCF level by 21775 cm^{-1}, it is evident that effectively only a small fraction of an electron is transferred in this transition. The first UV transition is found to have a larger oscillator strength than the visible ones, but the largest oscillator strengths are expected further into the UV.

(ii) Lactamase Models. Modeling the complete first shell of the active site using imidazole as histidine models is not feasible at this time. To determine whether a smaller model could provide meaningful results, test calculations were done on only the CA side of the enzyme. The histidines on the CA side were modeled by four analogues of decreasing complexity: imidazoles, imines, amides, and ammonias. The site models included three of these model histidines, a hydroxide, and a Co(II). The positions of the hydroxide oxygen and the histidine model nitrogens that are coordinated to the cobalt were all obtained from the crystal structure of the lactamase of *B. fragilis* (1znb). The resulting electronic transitions were nearly identical for all four models of histidine (Table 3). On the basis of these data, ammonia was chosen to be the histidine model in the full active-site calculations.

To estimate the spectral shifts that would result from adding electron correlation in the spd shells of the metal and the ligand orbitals, the model calculation with ammonia ligands using the MCQDPT method was repeated, incorporating charge-transfer states in addition to the 10 arising from the F and P states of cobalt (Table 4). The red shift in the MCSCF excitation energy for the visible transitions from state 8 to state 10 with the correlation correction derived from Table 4 is remarkably similar to that found for these states for the five-coordinate system with the methyl sulfide ligand (Table 2). These shifts are used to correct the visible transition energies calculated in the complete model.

The final two-site models of the lactamase active site are shown in Figure 2. All heavy-atom positions were obtained from the crystal structure of the *B. fragilis* lactamase (1znb). Hydrogen positions were optimized. The water hydrogen positions were set to the optimized hydrogen positions of the active-site model, where the histidines were modeled as imidazoles (Figure 1). The resulting excited-state energies and oscillator strengths are shown in Table 5. There is a shift to the red in the charge-transfer transitions of the aspartic acid model. However, this shift is not enough to distinguish between the two models, given the uncertainties in the calculations. On the other hand, the calculated spectrum with the cobalt on the CA side is substantially different from the spectrum with cobalt on the cysteine side. The CA visible transitions are to the red of models with the cobalt on the cysteine side and have oscillator strengths an order of magnitude stronger. The charge-transfer states from the CA side are too high in energy to be observed experimentally. These results clearly suggest that the experimentally observed visible transitions are dominated by contributions from the cobalt-substituted CA side of the active site, while

Table 2. Excited-State Energies for Methyl Sulfide−Water−Co^{2+} Complexes[a]

	six-coordinate			five-coordinate			four-coordinate		
state	MCSCF	MCQDPT	OS	MCSCF	MCQDPT	OS	MCSCF	MCQDPT	OS
2	446	406	0.000 00	2 009	3 152	0.000 005	1 775	5 504	0.000 001
3	691	1 336	0.000 00	2 242	3 667	0.000 006	2 745	7 676	0.000 005
4	5 007	7 239	0.000 00	2 635	4 061	0.000 000	3 827	8 542	0.000 003
5	5 100	7 646	0.000 00	3 400	4859	0.000 001	4 432	9 006	0.000 009
6	5 733	8 372	0.000 05	7 150	9 808	0.000 003	4 550	9 841	0.000 004
7	11 105	14 991	0.000 00	7 512	10 434	0.000 002	6 393	13 812	0.000 013
8	21 597	20 378	0.000 01	21 408	19 457	0.000 013	20 565	20 207	0.000 150
9	22 984	21 996	0.000 01	21 666	19 918	0.000 002	21 506	20 852	0.000 049
10	23 368	22 758	0.000 08	22 507	21 195	0.000 012	22 686	23 835	0.000 097
11	37 338	34 276	0.001 87	36 192	32 360	0.006 480	32 553	31 926	0.003 158
12	37 601	34 570	0.026 98	37 658	34 035	0.021 624	34 070	33 376	0.000 168
13	37 917	34 947	0.015 16	37 827	36 686	0.009 525	34 292	35 622	0.032 015
14	38 712	35 573	0.005 66	38 288	37 361	0.001 026	35 184	36 308	0.000 694
15	39 089	35 889	0.258 18	38 989	37 492	0.000 011	35 984	38 481	0.000 016
16	39 534	36 247	0.403 73	39 421	37 584	0.001 349	36 256	39 708	0.000 132
17	40 857	36 563	0.005 00	39 698	38 067	0.000 854	36 513	41 010	0.000 258

[a] The six-coordinate complex has five waters and a methyl sulfide coordinated to the cobalt ion. The five-coordinate complex has four waters and a methyl sulfide, and the four-coordinated complex has three waters and a methyl sulfide coordinated to the cobalt ion. All calculations were done on fully optimized structures. Energies are in wavenumbers. OS = oscillator strength.

Table 3. Comparison of MCSCF Transition Energies of the CA Side of the Metallo-β-lactamase with Different Models for the Histidines[a]

	ammonia		amine	imine	imidazole	
state	MCSCF	OS	MCSCF	MCSCF	MCSCF	OS
2	3 648	0.000 000	3 643	3 299	3 700	0.000 001
3	3 696	0.000 002	3 742	3 716	3 752	0.000 002
4	4 375	0.000 002	4 110	3 791	4 081	0.000 002
5	6 375	0.000 024	6 254	6 001	6 199	0.000 024
6	6 510	0.000 030	6 494	6 133	6 418	0.000 031
7	9 170	0.000 005	9 202	8 861	8 680	0.000 004
8	18 748	0.000 194	18 642	18 490	18 677	0.000 175
9	21 650	0.000 102	21 552	21 464	21 454	0.000 116
10	22 976	0.000 129	23 052	22 722	22 881	0.000 142

[a] Energies are in wavenumbers.

Table 4. Comparison of MCSCF and MCQDPT Transition Energies of the CA Side of Metallo-β-lactamase with Histidines Modeled as Ammonias[a]

state	MCSCF	MCQDPT	state	MCSCF	MCQDPT
2	3 707	4 179	10	25 017	23 667
3	4 000	4 375	11	36 715	37 289
4	4 704	5 629	12	39 793	38 188
5	6 414	7 793	13	39 991	40 932
6	6 985	8 168	14	40 432	42 191
7	9 373	12 096	15	41 356	42 795
8	20 268	17 925	16	42 849	43 854
9	23 281	21 181	17	43 117	45 045

[a] Energies are in wavenumbers.

the UV transitions are generated entirely by the cysteine side, as is generally assumed.

Due to the neglect of correlation in the MCSCF calculations, the transition energies in Table 5 are shifted relative to experiment. These shifts are estimated from the model complex data in Tables 2 and 4. On the basis of the data in Table 2, the visible transitions are shifted to 548, 470, and 456 nm on the cysteine side and to 665, 584, and 538 nm on the CA side. The visible transitions from the cysteine side would be observable around 470 nm, while the stronger red bands from the CA side do resemble the spectra observed for both the *B. fragilis*[14] and *B. cereus*.[9−11] Figure 3 shows the superposition of the recent spectrum for *B. fragilis*[14] on the calculated spectra, where the calculated peaks have been shifted by the amount indicated by the electron correlation energy shifts on model compounds. The shifts were obtained by taking the difference between the MCSCF and the MCQDPT energies for each state.

Discussion

The spectrum of cobalt is influenced most strongly by the ligands that are coordinated to it. The use of the native zinc crystal structure as the basis for the spectroscopic calculations was justified by geometry optimizations done with cobalt instead of zinc, which showed that the coordination numbers predicted for zinc and cobalt agree. The spectroscopic calculations support the assumption commonly made in analyzing the experimental spectrum, that the strongest visible transitions are due primarily to the CA side and the UV transitions are charge-transfer transitions from the cysteine ligand. Moreover, the relative positions of the peaks are fairly well accounted for by the MCSCF calculations, although the correlation energy correction is required in order to correct the peak positions. The observed visible transitions in the zinc-β-lactamases are exceedingly similar to those of the high pH form of carbonic anhydrase.[15] Indeed, the similarity of the two spectra indicates that the complex environment of the protein, and in particular the other metal site or the nearby ionic second shell of residues, have little effect on the spectral properties of the first shell of the active site.

The spectroscopic calculations predict that the observed visible transitions result from the CA side and the UV transitions are from the cysteine side. The visible spectrum from the cysteine side is not only much weaker than that due to the CA side but is also shifted significantly to the blue, with only one overlapping band between the two spectra. A more significant prediction can be made of the extent and intensity of the charge-transfer (UV) bands. Since the ground state of Co(I) is an F state and a number of degenerate atomic states have low excitation energies, a large number of charge-transfer excited states are expected.[22] On the basis of the correlation energy correction to the MCSCF excitation energies in Table 5, the first two charge-transfer states, 11 and 12, are predicted at 320 and 313 nm. Since the half-width of the experimental charge-transfer band at 340 nm is about 25 nm, the theoretical results imply that the band observed at 340 nm for *B. cereus* consists of the first two calculated transitions. The oscillator strength of

(22) National Bureau of Standards. *NBS Atomic Spectral Tables*; U.S. Government Printing Office: Washington, DC, 1952; Circular 467.

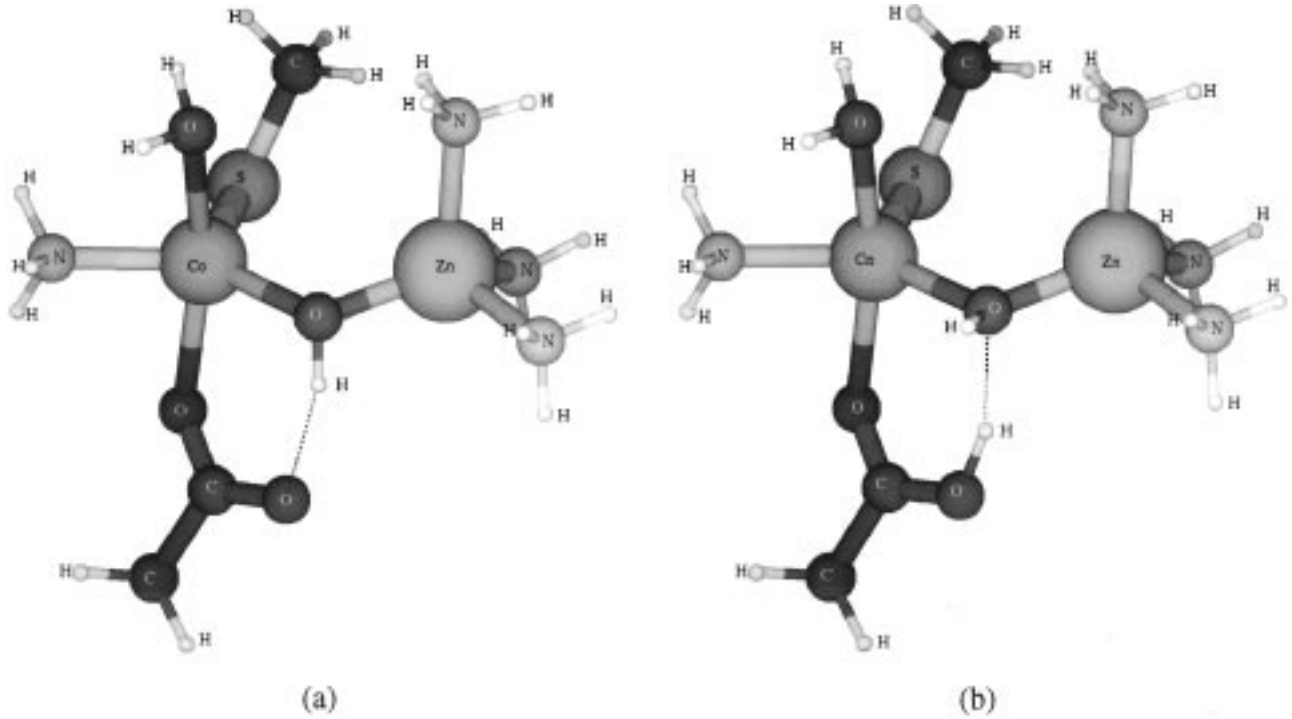

Figure 2. Active-site models used in calculations: (a) aspartate and (b) aspartic acid. The mages were generated with Molden.[27]

Table 5. Calculated Spectra of Active-Site Models of Co(II) β-Lactamases[a]

	Co on cysteine side					
	aspartate		aspartic acid		Co on CA side	
state	MCSCF	OS	MCSCF	OS	MCSCF	OS
2	1 824	0.000 001	2 068	0.000 007	1 544	0.000 000
3	2 071	0.000 007	2 245	0.000 001	1 667	0.000 001
4	3 218	0.000 027	2 908	0.000 030	2 437	0.000 000
5	4 567	0.000 004	4 120	0.000 003	3 457	0.000 013
6	6 655	0.000 006	6 836	0.000 007	3 930	0.000 009
7	8 863	0.000 003	8 320	0.000 003	5 802	0.000 005
8	20 294	0.000 011	20 274	0.000 007	17 372	0.000 183
9	23 016	0.000 046	22 622	0.000 074	19 236	0.000 094
10	23 224	0.000 008	23 057	0.000 021	19 925	0.000 148
11	35 110	0.001 260	33 481	0.006 536	44 839	0.000 804
12	35 613	0.000 191	34 354	0.000 035	45 078	0.001 228
13	35 844	0.007 689	34 720	0.009 733	50 695	0.000 040
14	36 518	0.000 217	34 786	0.000 595	51 795	0.000 021
15	36 796	0.006 197	35 267	0.004 546	53 329	0.000 005
16	37 396	0.006 694	35 908	0.010 073	61 457	0.000 775
17	37 934	0.000 034	36 238	0.000 528	62 645	0.000 554
18	39 308	0.006 628				
19	39 608	0.000 031				
20	39 771	0.000 083				
21	39 972	0.000 330				
22	40 621	0.000 031				
23	40 973	0.000 109				
24	41 194	0.000 677				
25	41 746	0.001 417				
26	42 120	0.009 920				
27	43 590	0.009 027				
28	42 968	0.002 203				
29	43 644	0.003 428				
30	43 794	0.000 058				

[a]Energies are in wavenumbers.

these charge-transfer bands is calculated to exceed the visible transitions from the CA side by a factor of 30. The next three transitions, which would span 280 nm, where tryptophan also absorbs, are an order of magnitude more intense and in qualitative agreement with the rapid increase in spectral intensity observed at 300 nm.[11]

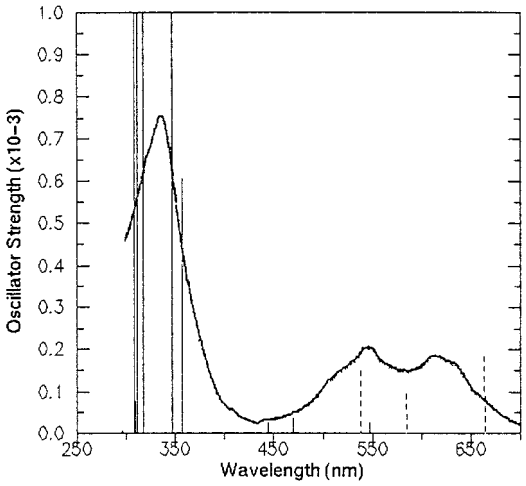

Figure 3. Superposition of the shifted calculated spectra and the experimentally obtained spectrum from *B. fragilis*.[14] Dashed lines are from the CA side Co(II), and solid lines are from the cysteine side Co(II).

The charge-transfer bands extend far into the UV (see Table 5). These bands appear to be more sensitive to environment than the visible bands. The calculations indicate that the protonation of the aspartate in the first shell shifts the transitions to the red by about 1500 cm^{-1}. It may be possible, therefore, to see differences in the protein environment of the active site between the different lactamases that cannot be seen in the visible region by studying the UV spectrum in the region of 200−400 nm. These transitions also overlap the tryptophan absorbance. Thus, it should be possible to detect fluorescence energy transfer between the cobalt on the cysteine side and the nearby tryptophans. Some fluorescence studies[11] have already found that the addition of cobalt quenches tryptophan fluorescence when added to the apo-enzyme or the sodium-bound enzyme. To a much smaller extent, zinc also quenches tryptophan fluorescence. Quenching can occur by radiative transfer to the charge-transfer bands that overlap the emission or by

electron transfer from the excited tryptophan to the open-shell cobalt cation. Since fluorescence quenching is dependent on the distance between the tryptophan residue(s) and the cobalts, fluorescence studies may also be a useful way to probe differences in the active-site environments of different lactamases.

Although the spectra of zinc-β-lactamase from *B. fragilis* and *B. cereus* now appear to be the same, there are variations in the spectra as cobalt is added to the apo-enzyme.[9,11,14] For *B. fragilis*, the simultaneous development of the visible and the UV transitions as cobalt was added to the apo-protein[14] was interpreted to mean that both metal sites initially have similar binding affinities for cobalt. The present calculations support this interpretation, since the observed visible transitions are from the CA side, while the UV can only come from the cysteine side. In contrast, the titration behavior of *B. cereus* is complicated.[9,11] It appears that the binding affinities of the two metal sites in the *B. cereus* are different from each other, whether measured by the activity of the enzyme or by fluorescence quenching. The strong metal binding site is thought to be the CA side, and the weak site is thought to be the cysteine side. That the CA side is the stronger binding site is suggested by the original crystal structure of the *B. cereus* lactamase,[23] which contains a single zinc in this site. There are two common features in the titration experiments for the *B. cereus*. First, the UV charge-transfer band is apparent even at very low cobalt concentrations. This indicates that the cobalt is binding to the cysteine side of the active site, because no charge-transfer bands in the near-UV originate from the CA side. Second, when one cobalt is added to the mono-zinc enzyme, a UV charge-transfer band appears with only weak absorption in the visible region. This suggests that the CA side binds zinc more tightly than the cysteine side. These interpretations are in conflict only if one assumes that zinc and cobalt have the same binding affinities for the two sites. Zinc and cobalt, however, do have different binding properties. Zinc prefers to be four-coordinate, while the open-shell nature of cobalt allows charge transfer from the ligands to the metal, giving cobalt the ability to more readily stabilize additional ligands.

The titration studies also suggest that the enzyme is active in the mono-zinc form, and there is evidence that the lactamases enzyme can function as a single zinc enzyme.[11,24] As previously mentioned, however, the crystal structure of the mono-zinc enzyme shows a solvent molecule in the second zinc site.[5] This solvent molecule may well be a sodium ion. It has been shown that the binding of cobalt is weaker in the presence of sodium, indicating that cobalt and sodium may compete for the same site.[9] If this is the case, then the models used to extract the cobalt and zinc binding affinities must include these competitive interactions with other metal ions. It is important to know whether the enzyme can, in fact, function with a single zinc in the absence of sodium and other cations in order to elucidate the enzyme mechanism.

The structural calculations reported here are limited to what was necessary to analyze the spectrum of the cobalt-substituted two-metal enzyme. Interpretation of the spectral properties when only a small amount of metal is present was done in terms of what is known for the bimetallic active site. However, the structure of the site with only a single transition metal or the site in early formation may be different. Further explorations of the active-site structure of zinc lactamase, at and away from the equilibrium structure, are underway. Such calculations are necessary to further interpret the confusing titration data and to explore the differences in structure and function between the lactamases from *B. cereus* and *B. fragilis*. The effect of the protein environment and ionicity on the active site structure will also be studied.

Acknowledgment. We gratefully acknowledge Drs. Nestor Concha, Osnat Herzberg, and Michael K. Gilson for insightful conversations, Drs. Michael Schmidt and Jan Jensen for help with the GAMESS code, and Dr. Walter Stevens for his careful reading of and comments on the manuscript. This work was supported by the National Institutes of Standards and Technology. The contents of this publication do not necessarily reflect the views or policies of the National Institute of Standards and Technology (NIST). Certain commercial equipment, software, instruments, and materials are identified in this paper in order to specify the experimental procedure as completely as possible. In no case does this identification imply a recommendation or endorsement by the National Institute of Standards and Technology, nor does it imply that the material, instrument, or equipment identified is necessarily the best available for the purpose.

JA990459X

(23) Carfi, A.; Pares, S.; Duée, E.; Galleni, M.; Duez, C.; Frère, J. M.; Dideberg, O. *EMBO J.* **1995**, *14*, 4914−4921.

(24) Paul-Soto, R.; Hernandez-Valladares, M.; Galleni, M.; Bauer, R.; Zeppezauer, M.; Frere, J. M.; Adolph, H. W. *FEBS Lett.* **1989**, *438*, 137−140.

(25) Humphrey, W.; Dalke, A.; Schulten, K. *J. Mol. Graphics* **1996**, *14.1*, 33−38.

(26) Merritt, E. A.; Bacon, D. J. *Methods Enzymol.* **1997**, *277*, 505−524.

(27) Schaftenaar, G. QCPE619, MOLDEN: A Portable Electron Density Program. *QCPE* **1992**, *12*, 3.